Study of Photocarrier Generation Mechanism in Bisazo Pigments from 1,5-Diaminoanthraquinone by Electron Spin Resonance

Zhongping Huang,* Guoping Wang, and Qingsen Yu

Department of Chemistry, Zhejiang University, Hangzhou, The Peoples's Republic of China 310027

Jinhong Pan

Department of Chemistry and Biochemistry, Worcester Polytechnic Institute, Massachusetts 01609

Received: September 21, 1999; In Final Form: February 6, 2000

The electron spin resonance (ESR) technique was introduced to study the photocarrier generation mechanism in the dual-layered organic photoreceptors containing DEH in the carrier transport layer (CTL) and bisazo pigments synthesized by coupling 1,5-diaminoanthraquinone with various 2-hydroxy-3-anphthanlidies in the carrier generation layer (CGL). The results showed that the photocarrier efficiency strongly depended upon the spin concentration of the bisazo pigments under irradiation. The dependence was successfully elucidated by the reaction rates of photocarrier generation elementary processes.

Introduction

The dual-layered photoreceptor (see Figure 1), composed of the carrier generation layer (CGL) and the carrier transport layer (CTL), has been widely used in electrophotography because of its high photosensitivity and durability as compared to the single photoreceptor.[1−3] Its photocarrier generation process is supposed to include three successive processes.[4] (i) The exciton produced by photon absorption in the bulk of the CGL diffuses to the CGL/CTL interface; (ii) the exciton undergoes the photoinduced electron transfer to generate a geminate pair at the interface, and the geminate pair dissociates into a free electron and hole pair; (iii) the hole is transported to the surface of the photoreceptor. Many investigations showed that the first excited singlet state is the precursor state for the photocarrier generation in the first process.[5−7] The photocarrier generation occurs at the CGL−CTL interface, via the photoinduced electron transfer (ET).[8,9] Its transport efficiency relates to the oxidation potentials of the carrier generation material (CGM) and carrier transport material (CTM).[10−16] The CTM is thought to be a catalyst that diminishes the activation energy of the exciton dissociation (the lowest excited state). The hole transport process in the CTL is a redox process of the electric field driven chain between the neutral molecules and their ion radicals.[17,18] However, the overall pathways and elementary processes have not been clearly understood. Undoubtedly, adequate knowledge of the photocarrier generation mechanism is necessary to search for excellent photoconductive materials.

The electron spin resonance technique was our new attempt to study the details of the carrier photogeneration processes. The idea is based on the CGMs being easily excited to generate electron−hole pairs under irradiation. Since the ESR is more sensitive to radicals than any other available technique,[19] it is used to study the electron−hole pairs. A quantitative relationship between the spin concentration and the average quantum efficiency, in case of a series of bisazo pigments, was uncovered. To verify the results, a kinetic investigation based on the elementary processes was involved.

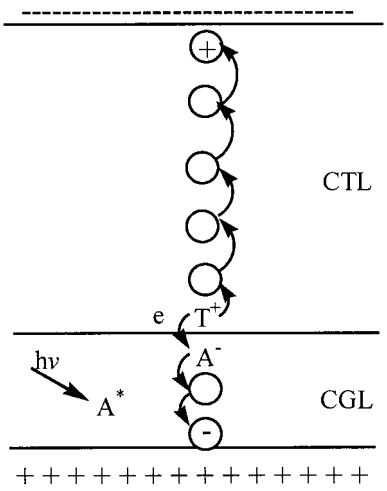

Figure 1. Schematic illustration of the photocarrier generation at the interface of the dual-layered photoreceptor. A and T, respectively, denote bisazo pigment and CTM molecule, and A* means the photoexcited bisazo pigment.

Experimental Section

(a) Materials. 1,5-Diaminoanthraquinone was purchased from Tokyo Kasei (Tokyo, Japan). The 2-hydroxy-3-naphthanlide couplers used were supplied by the Ninth Dye Co. (Shanghai, China) and were recrystallized from *N*,*N*-dimethylformamide (DMF) and methanol. *p*-(Diethylamino)benzaldehyde diphenylhydrazone (DEH) was synthesized for our experiment.[20]

(b) General Techniques. Melting points were taken on a precision melting apparatus of X6 Model and were uncorrected. Elemental analyses were performed on a Carlo. Erba. Infrared spectra were determined on a Daojin IR-470 Model. Absorption spectra were recorded on a BECKMAN-DU 50 UV−vis. Mass spectra were determined on a HEWLETT 5890. The bisazo pigments were measured by FAB mode, while DEH was measured by EI mode.

ESR spectra were determined on a JES-FEIXG ESR spectrometer (JEOL) with a xenon lamp. The xenon lamp emits

10.1021/jp9933727 CCC: $19.00
Published on Web 07/14/2000

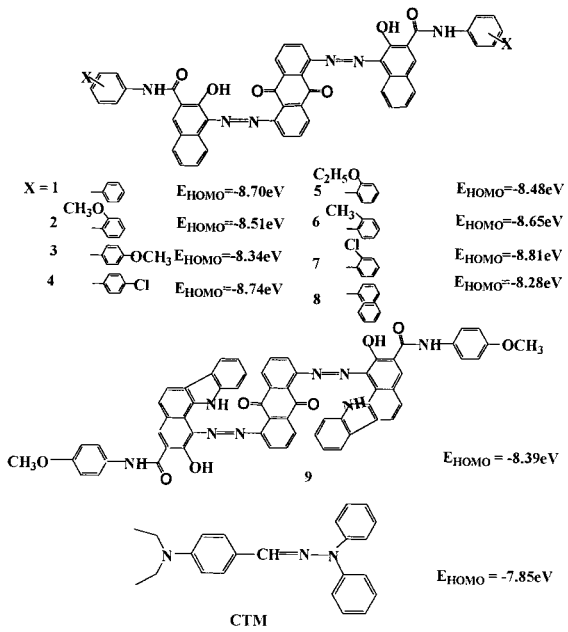

Figure 2. Molecular structures and the highest occupying molecular orbital (HOMO) energy levels of CGM and CTM.

ultraviolet light and white light, a monochromatic light of 569 nm was obtained by the filter which was fixed on the light access from the Xenon lamp to sample cell. The standard sample is diamond. The internal standard sample is manganese. The measurement was carried out under a magnetic field of 3300 ± 250 G and an oscillator frequency of 9.235 GHz.

(c) Synthesis of Bisazo Pigments. Nine bisazo pigments (see Figure 2) studied in this work were synthesized by first diazotizing 1,5-diaminoanthraquinone with a slight excess of sodium nitrite in 18 wt % of hydrochloric acid and then by coupling the resulting tetrazonium salt with various 2-hydroxy-3-anphthanlidies in DMF in the presence of sodium acetate. The crude pigments were isolated by filtration and were purified by repetitive washings with water and DMF to remove inorganic and organic impurities. All synthetic bisazo pigments are high-melting solids with unnoticeable melting or decomposition below 300 °C. Schematics of the synthesis are found in the literature.[21,22] Satisfactory elemental analytical and spectroscopic data were obtained from all bisazo pigments.

(d) Device Fabrication and Evaluations. The xerographic properties of bisazo pigments were examined in the dual-layered photoreceptors, which are composed of CGLs with various bisazo pigments and a CTL with the same CTM (DEH was used here). The CTL is about 18 μm in thickness and contains 40 wt % of DEH in a polycarbonate matrix. The CGL is about 0.7 μm, and the concentration of the bisazo pigment in the poly(methyl methacrylate) (PMMA) is 66.7 wt %. The geometry of all xerographic devices examined is held to be the same, thus enabling the xerographic properties of various bisazo pigments to be comparative.

The average quantum efficiency of the photoreceptor was measured by the above apparatus, which is schematically shown in Figure 3. The application of corona charge and subsequent exposure of the photoreceptor to light were conducted in an electrostatic paper analyzer, which consists of a corona generating unit, a tungsten lamp as the light source, and an electrostatic voltmeter. A monochromatic light of 569 nm was applied to the photoreceptor from the CTL side through an interference filter. The data of the decrease in the surface potential were fed to a computer through a preamplifier and an A/D converter to

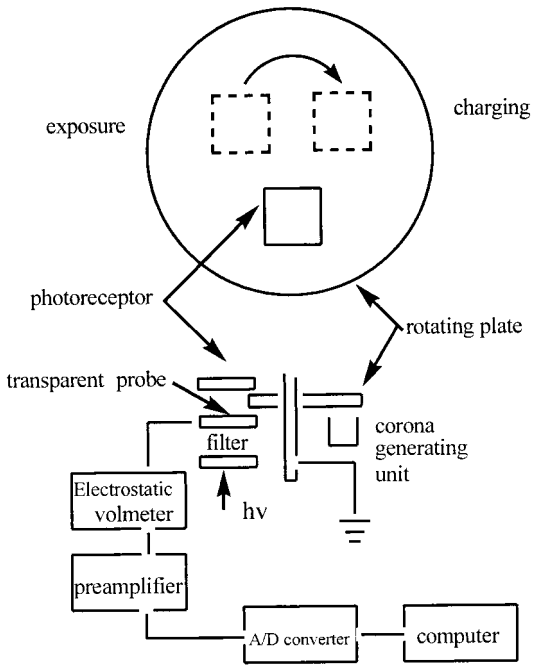

Figure 3. Schematic diagram of the experimental apparatus for average quantum efficiency measurement.

obtain the average quantum efficiency ($\bar{\eta}$), which was defined as the number of the surface charges neutralized by the absorbed photons within the time interval ($t_{1/2}$) from the initial potential (V_1) to $0.5V_i$. The value of $\bar{\eta}$ is given by

$$\bar{\eta} = \frac{\epsilon\epsilon_0 hC\Delta V}{el\lambda}\frac{1}{I't_{1/2}} \quad (1)$$

where ϵ is the dielectric constant of the photoreceptor medium (here, we used 3.0 as the dielectric constant, which was also adopted by Goliber[23]), ϵ_0 is the permittivity of free space, h is the Planck constant, C is the light speed, ΔV is half of the initial potential (V_i), l is the thickness of photoreceptor ($l = 18$ μm), λ is the light irradiation wavelength ($\lambda = 569$ nm), and I' is the incident light intensity per unit area. This equation was deduced from the quantum efficiency equation.[8,24]

(e) AM1 Calculation. The HOMO energy level calculations were carried out using Hyperchem 4.5 (AM1 method used here).[25]

Results and Discussion

Under the xenon lamp, 569 nm irradiation and no irradiation, the ESR signals of all bisazo pigments are single peaks found in the middle of two peaks of manganese. Their g factors are 2.0032, similar to that of α,α′-diphenyl-β-picrylhydrazyl.[26] The intensity of the ESR signal under irradiation is stronger than that without irradiation (see Figure 4). The ESR signal under irradiation is attributed to the photocarrier, in which the photocarrier generation mechanism is similar to that of the single layer photorecepor. The ESR signal without irradiation may arise from the intramolecular electron transfer or thermal effect**.** The enhancement in signal intensity under the xenon lamp is obviously larger than that under 569 nm. The reason is that the light intensity of 569 nm was much weaker than that of the light original source (or the xenon lamp) without through the filter.

Figure 5 shows the relationship between the spin concentration of sample **9** and the irradiation time. The result shows that as the irradiation time is increased from 1 to 3 min, the spin

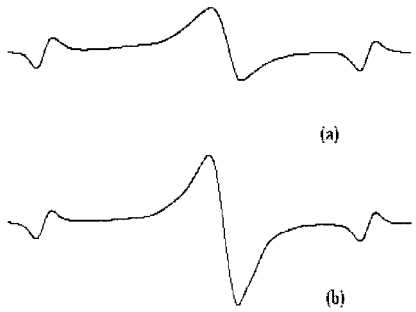

Figure 4. Electron spin resonance spectra of the manganese internal standard (lying in two sides of the plot) and sample **9** (middle peak lying in the middle of the plot): (a) without irradiation; (b) under the xenon lamp irradiation.

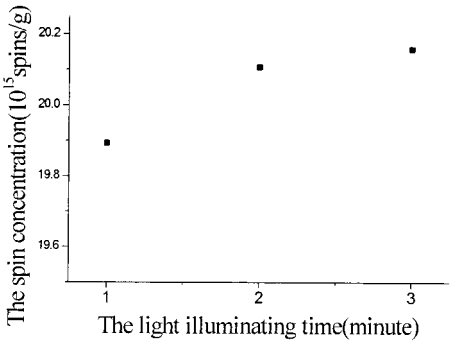

Figure 5. Spin concentration of sample **9** plotted as the function of the light irradiation time.

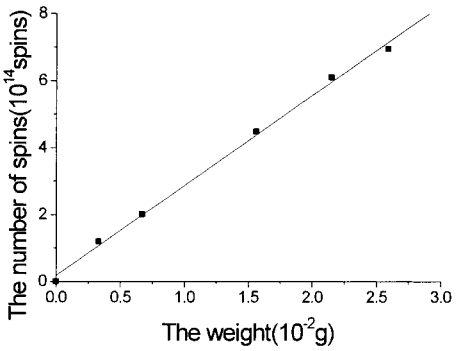

Figure 6. Spin numbers of sample **9** plotted as a function of the weight.

concentration increased slightly. The other bisazo pigments **1**−**8** show similar phenomena. The effect of irradiation time on the spin concentration was less. In the following experiments, the irradiation time was kept to 2 min.

To evaluate if the ESR spectrometer was quantitative, eight same-weight specimens from sample **9** were measured under the same condition. Their ESR results show the same spin concentrations. The relative error is less than 1%. In addition, the spin numbers of six specimens with different weights from sample **9** were measured (note: the empty tube has no ESR signal). The linear relationship between the spin number and the weight was excellent (see Figure 6). These phenomena indicate that this spectrometer is quantitative.

Many investigations showed that the photoreceptors using bisazo pigments as CGMs are extrinsic ones.[27] According to the Noolandi and Hong photogeneration model[10] (see Figure 7), the quantum efficiency of photogeneration is independent of the excitation wavelength for the extrinsic photogenerators. The photons from the light sources with the different excitation wavelengths lead to the excitons located in the different excited states. Therefore, the relationship between the spin concentration

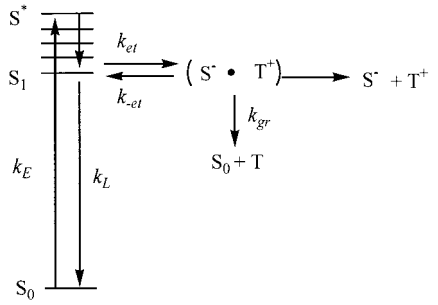

Figure 7. Schematic of the extrinsic carrier generation pathways in the layered photoreceptor containing the bisazo pigments.

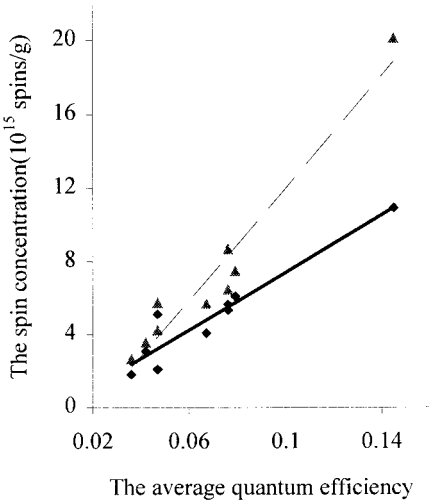

Figure 8. Spin concentration plotted as a function of the average quantum efficiency: (△) xenon lamp (♦) 569 nm irradiation.

TABLE 1: Average Quantum Efficiency of Pigments

no.	av quantum efficiency
1	0.047
2	0.076
3	0.042
4	0.079
5	0.047
6	0.067
7	0.036
8	0.076
9	0.145

and the average quantum efficiency was studied. The average quantum efficiency versus the spin concentration with irradiation is plotted in Figure 8, which shows a linear relationship. The correlation coefficients are respectively 0.97 (under xenon lamp) and 0.95 (569 nm irradiation). The linear relationship between the average quantum efficiency and the spin concentration under irradiation indicates that the spin concentration can show the overall photocarrier generation of the photoreceptors. The results also verify the above assumption that the photocarrier generation process for the different light sources is the same. There is no linear relationship between the average quantum efficiency and the spin concentration without irradiation (Table 1).

Next, the relationship between the neutralization rate of the surface charge of the photoreceptor and an incident light intensity was measured in order to investigate the bimolecular recombination process of the free carriers. In the case that the recombination rate of the carriers is negligibly low, the neutralization rate of the surface charge is proportional to the incident light intensity. Conversely, in the case that the bimolecular recombination of carriers predominantly occurs, the

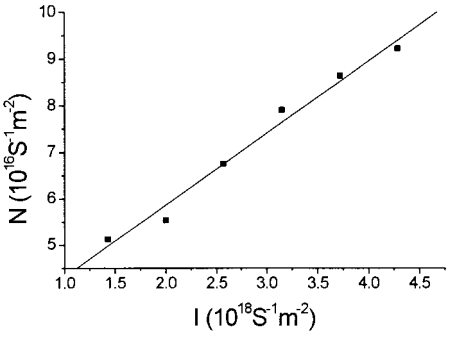

Figure 9. Neutralization rate for the surface charge N versus illumination rate of incident light I for the dual-layered photoreceptor. The electric fields were at 2.2×10^7 V m^{-1}.

neutralization rate should be proportional to the square root of the incident light intensity.[28] The average neutralization rate per unit area within time, or $t_{1/2}$, can be expressed by

$$N = \frac{\epsilon\epsilon_0 hC\Delta V}{el\lambda}\frac{1}{t_{1/2}} \tag{2}$$

The relationship between N and incident light intensity, I, is shown in Figure 9. It is deduced that the bimolecular recombination rate is negligibly small. Accordingly, once the free carriers are generated at the interface, the holes among them inject into the CTL and transport to the surface of the photoreceptor effectively to compensate the surface charges, and a substantial bimolecular recombination of the free carriers does not occur.

The above observations are summarized as follows: the bisazo pigment is first transited to the higher excited state by absorption of photons in the bulk of the CGL. The exciton in the higher excited state (S*) relaxes to the lowest excited state (S_1). The exciton diffuses to the bisazo−CTM interface to generate ET, which forms a geminate pair ($S^-\cdot T^+$). The geminate pair dissociates into the free carriers or undergoes geminate recombination. The free carriers neutralize the surface charges of the photoreceptor and never undergo bimolecular recombination. These are the whole processes of the extrinsic photocarrier generation. Since the exciton diffusion rate is fast enough in the overall processes, the exciton diffusion process is not a rate-determining step. Thus, we concentrate on consideration of the other elementary processes.

Because the photoinduced discharge of the surface potential is emission-limited under the experimental conditions,[29] the steady states are postulated to be the intermediates of S_1 and ($S^-\cdot T^+$). Thus, the overall photocarrier generation rate constant, k_s, is expressed as

$$k_s = \frac{k_E k_{diss} k_{et}}{k_L k_{diss} + k_L k_{-et} + k_L k_{gr} + k_{et} k_{diss}[T] + k_{et} k_{gr}[T]} \tag{3}$$

When the geminate pair can generate the free carriers effectively at the electric field, $k_{diss} \gg k_{gr}$ and $k_{diss} \gg k_{-et}$ are assumed. Thus, eq 3 is simplified to

$$k_S = \frac{k_E k_{diss} k_{et}}{k_L k_{diss} + k_{et} k_{diss}[T]} \tag{4}$$

Now we consider the case of $k_{et} \gg k_L$. When $k_{et} \gg k_L$, eq 4 is simplified to

$$k_s = k_E/[T] \tag{5}$$

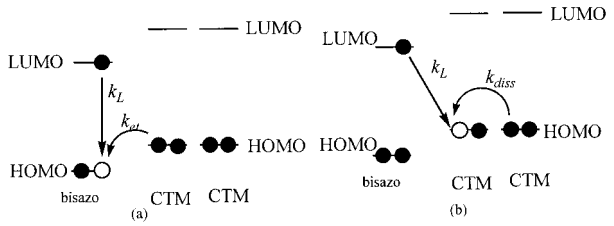

Figure 10. Schematic energy diagram of the simplified extrinsic photogeneration expressed by four elementary processes: (a) geminate hole−electron pair generation process, the geminate-pair generation (charge separation) competing with the deactivation of the excited state; (b) free carrier generation process, the geminate-pair dissociation (charge transfer) competing with the geminate-pair recombination (charge recombination).

Because $k_{diss} \gg k_{gr}$ and $k_{diss} \gg k_{-et}$ have been presumed, it means that the generation efficiency of the free carriers from the geminate pairs equals unity under higher electric fields. Under this condition, the quantum field of the overall photocarrier generation is defined by[30]

$$\eta = \frac{k_S}{k_S + k_L} \tag{6}$$

Substituting eq 5 into eq 6, one obtains

$$\eta = \frac{k_E}{k_E + k_L[T]} \tag{7}$$

Because the quantum efficiency of the photoreceptor was measured by using the same kind of CTM with the same DEH content, the concentration of [T] in eq 7 is the same. It is, therefore, suggested that the quantum efficiency of the overall photocarrier generation strongly depend on the CGMs.

$k_{et} \gg k_L$ means that the electron in the HOMO of the ground state of CTM injects into the hole much faster than that in the LUMO of the photoexcited state of CGM (see Figure 10a). According to the Marcus's expression of the electron transfer,[28]

$$k_{et}/k_{-et} = \exp(\Delta E/k_B T) \tag{8}$$

ΔE is the difference between the HOMO energy levels of CTM and CGM.

$$\Delta E = E_{HOMO}(CTM) - E_{HOMO}(CGM) \tag{9}$$

When the HOMO energy level of CGMs is lower than that of CTM, the geminate-pair generation process is exothermic ($\Delta E > 0$).[28] The exothermic process benefits the enhancement of the geminate-pair generation rate. The AM1 calculation show that the HOMO energy levels of all bisazo pigments are lower than that of CTM (DEH was used here) (see Figure 2). The geminate-pair generation process of all bisazo pigments is exothermic, and thus the geminate-pair generation rate is fast. Since the geminate-pair generation and deactivation are two competitive processes (see Figure 10a), the fast geminate-pair generation rate means that the geminate-pair deactivation rate is relatively slow. k_{gr} is regarded as the rate constant of charge recombination. When the energy difference is zero ($\Delta E = 0$), k_{diss} is considered to be the charge transfer and strongly depends on electric field.[28] When the quantum efficiency of the photoreceptor was detected under the high electric field (2.2×10^7V/m), the charge transfer is fast. Since the charge transfer and charge recombination are two competitive processes (see Figure 10b), the fast charge transfer means that the charge recombina-

tion rate is relatively slow. In addition, when $\Delta E = 0.40$ eV, the magnitude of k_{et}/k_{-et} is calculated to be 5.8×10^6. The smallest ΔE among these bisazo pigments is equal to 0.43 eV (sample **8**). This obviously reveals that the geminate-pair generation takes place predominantly, while the substantial back-process does not occur. Therefore, the photocarrier generation of these bisazo pigments may fit the condition for eq 7 ($k_{et} \gg k_L$, $k_{diss} \gg k_{gr}$, and $k_{diss} \gg k_{-et}$). This means that the quantum efficiency of the photoreceptor strongly depends on CGM. The spin concentration measured under magnetic field and light irradiation can display the photocarrier generation of bisazo pigments. Thus, the linear relationship between the spin concentration and the average quantum efficiency was understood without difficulty.

Conclusions

In the case of a series of bisazo pigments synthesized from 1,5-diaminoanthraquinone, the quantitative relationship between the average quantum efficiency and the spin concentration measured under irradiation was shown. Then, the quantum efficiency of the overall photocarrier generation was investigated by the kinetic method, which uses the rate constants of the elementary processes. The linear relationship between the average quantum efficiency and spin concentration was explained by the equation obtained from the above kinetic investigation. This is a strong indication that ESR is another efficient method to investigate the details of the photocarrier generation process for the organic photoconductive materials.

Acknowledgment. The authors acknowledge Dr. Sonia Glazer and Dr. Francine Smith for their help in modification.

Appendix: Derivation of Equation 3

Because the photoinduced discharge was measured under the emission-limited condition, the concentration of the intermediate in Figure 9, S_1 is presumed to be the steady state. Thus, a concentration change in term of rate is given as

$$d[S_1]/dt = k_E[S_0] - k_L[S_1] - k_{et}[S_1][T] + k_{-et}[(S^-\cdot T^+)] = 0 \quad (A1)$$

k_E represents the S_1 generation rate constant, k_L represents the S_1 deactivation rate constant, k_{et} represents the geminate-pair generation rate constant, and k_{-et} represents the rate constant of its corresponding reverse process.

For the other intermediate, $(S^-\cdot T^+)$,

$$\frac{d[(S^-\cdot T^+)]}{dt} = k_{et}[S_1][T] - (k_{diss} + k_{-et} + k_{gr})[(S^-\cdot T^+)] = 0 \quad (A2)$$

k_{diss} represents the geminate-pair dissociation rate constant, and k_{gr} represents the geminate-pair recombination rate constant.

The overall photocarrier generation rate constant, k_S, is expressed by

$$k_S[S_0][T] = k_{diss}[(S^-\cdot T^+)] \quad (A3)$$

From eqs A1 and A2, $[S_1][T]$ could be eliminated as

$$k_E[S_0][T] - \frac{k_L(k_{diss} + k_{-et} + k_{gr})}{k_{et}[T]}[(S^-\cdot T^+)] - (k_{diss} + k_{gr})[(S^-\cdot T^+)] = 0 \quad (A4)$$

According to eqs A3 and A4, A5 is induced.

$$\frac{k_E k_{diss}}{k_S[T]}[(S^-\cdot T^+)] = \left(\frac{k_L(k_{diss} + k_{-et} + k_{gr})}{k_{et}[T]} + k_{diss} + k_{gr}\right)[(S^-\cdot T^+)] \quad (A5)$$

After the concentration term, $[(S^-\cdot T^+)]$, is canceled from A5, the k_S expression is given as

$$k_S = \frac{k_E k_{diss} k_{et}}{k_L k_{diss} + k_L k_{-et} + k_L k_{gr} + k_{et} k_{diss}[T] + k_{et} k_{gr}[T]} \quad (3)$$

References and Notes

(1) Hashimoto, M. *Electrophotography* **1986**, *25*, 230.
(2) Sasaki, M. *Nippon Kagaku Kaishi* **1986**, *1986*, 379.
(3) Dipaola-Baranyl, G.; Hasiao, C. K.; Hor, A. M. *J. Imaging Sci.* **1990**, *34*, 224.
(4) Patsis, A. V.; Seaanor, D. A. *Photoconductivity in polymers*; Technomic: Westport, CT, 1976.
(5) Popovic, Z. D. *Chem. Phys*. **1984**, *86*, 311.
(6) Popovic, Z. D. *Chem. Phys. Lett.* **1983**, *100*, 227.
(7) Popovic, Z. D.; Hor, A. M.; Loutfy, R. O. *Chem. Phys*. **1988**, *127*, 451.
(8) Umeda, M.; Shimada, T.; Aruga, T.; Niimi, T.; Sasakj, M. *J. Phys. Chem.* **1993**, *97*, 8531.
(9) Niimi, T.; Umeda, M. *J. Appl. Phys*. **1993**, *74*, 465.
(10) Law, K. Y. *Chem. Rev*. **1993**, *93*, 449.
(11) Melz, P. J.; Champ, R. B.; Chang, L. S.; Chiou, C.; Keller, G. S.; Liclican, L. C.; Neiman, R. B.; Shattuck, M. D.; Weiche, W. J. *Photogr. Sci. Eng.* **1977**, *21*, 73.
(12) Law, K. Y.; Tarnawskyj, I. W. *J. Imaging Sci. Technol*. **1994**, *38*, 118.
(13) Kitamura, T.; Yokoyama, M. *J. Imaging Sci*. **1990**, *34*, 197.
(14) Menzel, E. R.; Popovic, Z. D. *Chem. Phys. Lett*. **1978**, *55*, 177.
(15) Pan, J. H.; Huang, Z. P.; Cai, G. Q.; Yu, Q. S.; Zong, H. X. *Chem. J. Chin. Univ*. **1998**, *19*, 1962.
(16) Huang, Z. P.; Pan, J. H.; Cai, G. Q.; Yu, Q. S.; Lin, R. S. *Acta Phys. Chim. Sin*. **1998**, *14*, 557.
(17) Kitamura, T.; Yokoyama, M. *J. Appl. Phys*. **1991**, *89*, 821.
(18) Stolka, M.; Yanus, J. F.; Pai, D. M. *J. Phys. Chem*. **1984**, *88*, 4707.
(19) Olsen, E. D. *Modern Optical Methods of Analysis*; McGraw−Hill: New York, 1975.
(20) Arita, T.; Mabuchi, M.; Umehara, S.; Sakai, K. *Ger. Offen. DE* **1984**, *3,331*, 259.
(21) Law, K.-Y.; Tarnawskyl, I. W. *J. Imaging Sci. Technol*. **1995**, *39*, 126.
(22) Law, K.-Y.; Tarnawskyj, I. W. *J. Imaging Sci. Technol*. **1993**, *39*, 1.
(23) Goliber, T. E.; Perlstein, J. H. *J. Chem. Phys*. **1984**, *80*, 4162.
(24) Borsenberger, P. M.; Ateya, A. I. *J. Appl. Phys*. **1978**, *49*, 4035.
(25) *HyperChem*, Release 4.5 for windows; Molecular Modeling System, Hypercube, Inc.: Gainesville, FL, 1994.
(26) Robison, J. W. *Practical Handbook of Spectroscopy*; CRC Press Inc.: Boca Raton, FL, 1991; p 677.
(27) Umeda, M.; Hashimoto, M. *J. Appl. Phys*. **1992**, *72*, 117.
(28) Umeda, M. *J. Imaginf Sci. Technol*. **1999**, *43*, 254.
(29) Umeda, M.; Nimi, T.; Hashimoto, M. *Jpn. J. Appl. Phys*. **1990**, *29*, 2746.
(30) Umeda, M.; Shimada, T.; Aruga, T.; Niimi, T.; Sasaki, M. *J. Phys. Chem.* **1993**, *97*, 8531.